Synthesis and Properties of Hydrophilic Segmented Block Copolymers Based on Poly(ethylene oxide)-ran-poly(propylene oxide)

A. C. IJzer,[1,2] A. Arun,[1,3]* S. R. Reijerkerk,[2] K. Nijmeijer,[2] M. Wessling,[2] R. J. Gaymans[1]

[1]*Synthesis and Technology of Engineering Plastics, Faculty of Science and Technology, University of Twente, 7500 AE Enschede, The Netherlands*
[2]*Faculty of Science and Technology, Membrane Science and Technology, Institute of Mechanics, Processes and Control Twente (IMPACT), University of Twente, 7500 AE Enschede, The Netherlands*
[3]*Dutch Polymer Institute, 5600 AX Eindhoven, The Netherlands*

Received 21 September 2009; accepted 4 December 2009
DOI 10.1002/app.31906
Published online 29 March 2010 in Wiley InterScience (www.interscience.wiley.com).

ABSTRACT: The present article discusses the synthesis and various properties of segmented block copolymers with random copolymer segments of poly(ethylene oxide) and poly(propylene oxide) (PEO-*r*-PPO) together with monodisperse amide segments. The PEO-*r*-PPO contained 25 wt % PPO units and the segment presented a molecular weight of 2500 g/mol. The synthesized copolymers were analyzed by differential scanning calorimetry, Fourier transform infra-red spectroscopy, atomic force microscopy and dynamic mechanical thermal analysis. In addition, the hydrophilicity and the contact angles (CAs) were studied. The PEO-*r*-PPO segments displayed a single low glass transition temperature, as well as a low PEO crystallinity and melting temperature, which gave enhanced low-temperature properties of the copolymer. The water absorption values remained high. In comparison to mixtures of PEO/PPO segments, the random dispersion of PPO units in the PEO segments was more effective in reducing the PEO crystallinity and melting temperature, without affecting the hydrophilicity. Increasing the polyether segment length with terephthalic groups from 2500 to 10,000 g/mol increased the hydrophilicity and the room temperature elasticity. Furthermore, the CAs were found to be low 22–39° and changed with the crosslink density. © 2010 Wiley Periodicals, Inc. J Appl Polym Sci 117: 1394–1404, 2010

Key words: segmented block copolymer; amide; monodisperse; poly(ethylene oxide); poly(propylene oxide)

INTRODUCTION

Thermoplastic elastomers based on segmented block copolymers display a two-phase morphology, with a continuous soft segment (SS) phase of low glass transition (T_g) and a melting transition of the hard segment (HS) phase at a high temperature.[1,2] The hard phase crystallites are the physical crosslinks of the low T_g soft phase segments and also acts as a filler for the soft phase.[1–4] In some cases, the SSs can also crystallize like with poly(ethylene oxide) (PEO) and then a three phase structure is obtained.[5] The PEO is sometimes also called or also called poly(ethylene glycol).

Copolymers with PEO segments are hydrophilic materials and such copolymers find applications in numerous fields, and for several of these applications, the low-temperature properties are crucial.

There exist several reports on PEO-based segmented block copolymers with rigid segments constituted of either urethanes,[6–11] esters,[12–15] or amides.[5,16–18] PEO segments demonstrate a low glass transition temperature (−40°C) and can easily undergo crystallization. PEO-containing segmented block copolymers present low contact angles(CAs) with water,[5,15–19] a high water vapor transport[20] and an elevated selective CO_2 transport.[14,16,17,21] However, the crystalline PEO phase if present reduces the low-temperature flexibility of the material.[5]

To improve these low-temperature properties, mixtures of PEO/PTMO or PEO/PPO segments have been studied.[6,7,18,22–25] A mixture of PEO/PTMO segments has been found to demonstrate the lowest PEO crystallinity at a 50/50*M* composition.[25] With a mixture of PEO/PPO segments, the crystallinity has been seen to decrease with the PPO content, and the lowest values were obtained at 50 mol % PEO or less.[18] PPO was thus more effective in reducing the PEO crystallinity than PTMO, and this was ascribed to the methyl side groups of

**Present address:* Government Arts College, Tiruvannamalai, Tamil Nadu, India.
Correspondence to: R. J. Gaymans (r.j.gaymans@utwente.nl).

Contract grant sponsor: Dutch Polymer Institute (DPI, The Netherlands), project #497.
Contract grant sponsor: European Union (FP6 integrated project NanoGLOWA); contract grant number: NMP3-CT-2007-026735.

propylene oxide hindering the crystallization. Relevant to this paper is a copolymer consisting of a mixture of PEO/PPO segments (81/19) presented a T_g at −45°C, a PEO T_m at 32°C and a heat of fusion of 64 J/g_{PEO}.[3,18]

To improve the effectiveness of the PPO segments with regard to disturbing the PEO crystallization, random prepolymers (PEO-*r*-PPO) of PEO and PPO units with only 25 wt % PPO units can be used instead of mixtures of segments. This article presents a study in line with this idea, with the addition of incorporating HSs consisting of monodisperse tetra-amide segments (T6T6T) based on terephthalic (T) and hexamethylene diamine[6] groups. These T6T6T segments have been found to crystallize fast and to high degrees, resulting in small quantities being dissolved in the polyether phase.[3,5] The T6T6T segments also present a high-melting transition that gives the copolymers a large useful temperature range. Hydrophilic PEO-T6T6T copolymers have been well studied.[5,19–26] With monodisperse HSs that crystallizes to a large extend, the structure of the copolymer is well defined.

It is also know that the chain mobility can be increased by increasing the ether segment length. By using terephthalic extender units, the segment length can be increased without demixing taking place.[26–29] Also, the presence of terephthalic extender units in the chain leads to a suppression of the PEO crystallinity.

This article describes the synthesis and a selection of properties of segmented block copolymers based on PEO-*r*-PPO_{2500} segments. The obtained results were compared to those from previous studies on PEO_{2000}-T6T6T[5] and PPO_{2300}-T6T6T.[3] Figure 1 displays the chemical structures of the segments used in the block copolymers.

The PEO-*r*-PPO_{2500} segments had a molecular weight of 2500 g/mol and a PPO concentration in the prepolymer of 25 wt %. The SS molecular weight was increased by extending the polyether segment with terephthalic groups ((PEO-*r*-PPO_{2500}-T)$_x$-PEO-*r*-PPO_{2500}). The effect of such an extension on the transitions and thermal mechanical behavior was investigated.

EXPERIMENTAL

Materials

N-methyl-2-pyrrolidone (NMP), phenol, 1,1,2,2-tetrachloroethane, hexafluoro isopropanol (HFIP), PEO-*r*-PPO_{1000}, and PEO-*r*-PPO_{2500} (i.e., with an M_n of 1000 and 2500 g/mol, respectively) were obtained from Aldrich. Also, the tetra-isopropyl orthotitanate (Ti(i-$OC_3H_7)_4$) catalyst was purchased from Aldrich and diluted in *m*-xylene (0.05*M*) from Fluka. The antioxidant Irganox 1330 was obtained from CIBA. The synthesis of diphenyl terephthalate and tetra-amide T6T6T-diphenyl has been described elsewhere,[3] as has the synthesis of PEO_{2000}-T6T6T.[5] The investigation also involved the synthesis of PPO_{2300}-T6T6T, with polypropylene oxide segments that were endcapped with 20 wt % ethylene oxide.[3]

Synthesis of the segmented block copolymers

Monodisperse polyamide block copolymers were synthesized by a polycondensation reaction using polyether segments (PEO-*r*-PPO_{2500}) and T6T6T-diphenyl tetra-amide units. The synthesis of PEO-*r*-PPO_{2500}-T6T6T is here given as an example. The reaction was carried out in a 250-mL stainless steel vessel equipped with a nitrogen inlet and mechanical stirrer. The vessel containing T6T6T-phenyl (6.48 g, 8 mmol), PEO-*r*-PPO_{2500} (20 g, 8 mmol), Irganox 1330 (0.20 g), and 50 mL NMP was heated in an oil bath to 180°C after which the catalyst solution was added (2.5 mL of 0.05*M* Ti(i-$OC_3H_7)_4$ in *m*-xylene). The stirred reaction mixture was heated to 180°C for 30 min, and the temperature was subsequently raised step-wise to 250°C within a time frame of one and a half hour. The reaction mixture was stirred at 250°C for 2 h after which the pressure was carefully reduced (P < 20 mbar) to distil off the NMP. The pressure was further reduced to <0.3 mbar for 1 h,

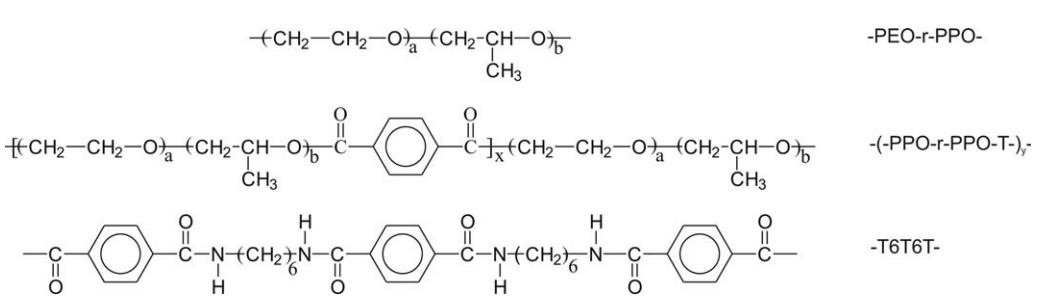

Figure 1 The chemical structures of the PEO-*r*-PPO and (PEO-*r*-PPO-T)$_y$ and the T6T6T segments used in the block copolymers.

and the reaction mass was then cooled slowly while maintaining the low pressure. The resultant copolymer was transparent with a yellowish hue. Before analysis, the polymer was dried overnight in a vacuum oven at 80°C

The (PEO-*r*-PPO-T)$_y$-T6T6T copolymers were synthesized in a similar way with the exception of part of the T6T6T-diphenyl being replaced by diphenyl terephthalate.

Viscometry

Viscometry was used to examine the molecular weights of the obtained polymers. Values of inherent viscosity (η_{inh}) were determined at 25°C using a capillary Ubbelohde type 0B viscometer. The polymer solution had a concentration of 0.1 g/dL in a 1 : 1 (molar ratio) mixture of phenol/1,1,2,2-tetrachloroethane.

Differential scanning calorimetry

Differential scanning calorimetry (DSC) was used to determine the melting and crystallization temperatures and enthalpies of the polyether block copolymers. Thermograms were recorded on a Perkin–Elmer DSC7 apparatus, equipped with a PE7700 computer and TAS-7 software. All samples were dried in a vacuum oven at 70°C overnight before use. The dried samples (8–12 mg) were heated from −90 to 200°C (to above the melting temperature) and subsequently cooled to be reheated at a rate of 20°C/min. The maximum of the endothermic peak in the second heating scan was used to determine the melting temperature (T_m).

Fourier transform infrared spectroscopy

Fourier transform infrared spectroscopy (FTIR) was used to determine the crystallinity of the amide segment. Infrared spectra were obtained with a Biorad FTS-60 spectrometer with a resolution of 4 cm^{-1}. The measurements were carried out at room temperature on samples prepared by adding a droplet of the block copolymers in HFIP solution (1 g/L) on a pressed KBr pellet. After evaporation of the solvent, a thin polymer film remained on the pellet on which the analysis was performed. The degree of crystallinity (X_c) of the rigid segments in the polymers could be estimated by using eq (1).

$$X_{c\ FT\text{-}IR} = \frac{\text{Crystalline amide peak}}{\text{Amorphous} + \text{Crystalline amide peak}} = \frac{\lambda_{25^oc\ (1627\ cm^{-1})}}{a \times \lambda_{25^oc(1660\ cm^{-1})} + \lambda_{25^oc(1627\ cm^{-1})}} \quad (1)$$

The heights of the amorphous and crystalline amide peaks were related by the factor "*a*" with a value of 2.4.[29]

Atomic force microscopy

Atomic force microscopy (AFM) measurements were carried out with a nanoscope IV controller (Veeco) operating in tapping mode. The AFM was equipped with a J-scanner with a maximum size of 200 μm^2. A TESP-cantilever (Veeco) was used and gentle tapping was applied to obtain the phase images. The amplitude in free oscillation was 5.0 V, and the operating set point value (A/A_o) was chosen to the relatively low value of 0.7. Scan sizes were 1–3 μm^2 to obtain the best possible contrast. The samples were prepared by solution casting. A 10 wt % solution of the copolymer in hexafluoroisopropanol (HFIP) was casted on silicon wafer with film thickness of ~ 20 μm and 100 μm thick.

Dynamic mechanical thermal analysis

The torsion behavior (storage modulus G' and loss modulus G'' as functions of temperature) was measured using a Myrenne ATM3 torsion pendulum at a frequency of 1 Hz and 0.1% strain. Before use, injection molded polymer samples (70 × 9 × 2 mm^3) were dried in a vacuum oven at 50°C overnight. Following this, samples were cooled to −100°C and subsequently heated at a rate of 1°C/min. The glass transition temperature (T_g) was defined as the temperature location of the maximum of the loss modulus, and the flow temperature (T_{flow}) was determined as the temperature where the storage modulus reached 0.5 MPa. The temperature at which the rubber plateau started was denoted the flex temperature (T_{flex}) and the storage modulus at 20°C was labeled $G'_{20°C}$.

Water absorption

The equilibrium water absorption (WA) was measured on pieces of injection-molded polymer bars. The samples were placed in a desiccator with demineralized water at the bottom for four weeks at room temperature. The WA was defined as the weight gain of the polymer according to eq. (2):

$$\text{water absorption} = \frac{m - m_0}{m_0} \times 100\%\ (wt\ \%) \quad (2)$$

where m_0 is the weight of the dry sample and m is the weight of the sample after conditioning to equilibrium.

The water concentration in the swelled copolymer (ϕ) was calculated according to eq. (3):

$$\phi = \frac{m - m_0}{m} \times 100\%\ (\text{wt}\ \%) \quad (3)$$

Contact angles

Static captive (air) bubble (CB) contact angle measurements were performed by introducing a 10-μL air

bubble from a microsyringe below the surface of a polymer film, which, in turn, was placed in an optical cuvette filled with demineralized water. The experiments were carried out at 22°C and a video-based Optical Contact Angle Meter OCA15 plus (DataPhysics Instruments) was used. Immediately after the air bubble was placed on the surface, CAs were calculated with a SCA202 software in manual evaluation mode. The results were averages of at least 20 measurements and the standard deviation in the CA was $\sim 4^{o}$.

RESULTS AND DISCUSSION

A series of hydrophilic copolymers based on PEO-*r*-PPO SSs and T6T6T HSs was studied. The T6T6T-diphenyl units, monodisperse in length, were prepared before the polymer synthesis and had a melting temperature of 316°C and the heat of fusion 129 J/g.[3] Copolymers of PEO-*r*-PPO_{2500} were compared with either PEO_{2000}[5] or PPO_{2300} segments.[3] The poly(propylene oxide) had EO end groups (20 wt %) (EO-*b*-PPO-*b*-EO)$_{2300}$ and was denoted PPO_{2300}.

In the second copolymer series, the molecular weight of the PEO-*r*-PPO SSs was increased from 1000 to 10,000 g/mol. The materials with molecular weights of 1000 and 2500 g/mol consisted of PEO-*r*-PPO segments, and the 3750–10,000 g/mol materials were -PEO-*r*-PPO_{2500}- segments extended with terephthalic groups (T) to -(PEO-*r*-PPO_{2500}-T)$_x$-PEO-*r*-PPO_{2500}-. These extended segments were denoted (PEO-*r*-PPO_{2500}-T)$_y$ and the subscript y stands for the molecular weight of that segment. The influence of the PEO-*r*-PPO SS length on the PEO crystallinity, the low temperature properties, the hydrophilicity, and the CAs was explored.

MATERIALS

The copolymers were synthesized with a high temperature melt polymerization starting from dihydroxy polyether segments and T6T6T-diphenyl ester. As T6T6T is a short unit (624 g/mol), its concentration in the copolymers was low—ranging from 40 down to 6 wt %. Even at such low T6T6T concentrations, the materials were solid at room temperature. The composition of the matrix phase was important for the WA, the surface characteristics, and the gas transport properties. Thus, in addition to the polyether concentration in the copolymer, also the PEO concentration in the ether phase was of considerable relevance.

Copolymers with PEO-*r*-PPO_{2500} segments

PEO has a regular structure and crystallizes easily. As a result, the copolymers displayed both a glass transition temperature and a melting temperature of the PEO segments.[5] On the other hand, PPO is amorphous because of its methyl side groups and the copolymers containing PPO thereby presented a low T_g and lacked a PPO melting temperature.[3] The PEO-*r*-PPO_{2500} segments consisted of PEO and PPO units that were randomly distributed in the chain. The polyether segments in the PEO_{2000}, PPO_{2300} and PEO-*r*-PPO_{2500} had all similar molecular weights (2000–2500 g/mol) and thus also similar T6T6T concentrations (20–24 wt %). The properties of these copolymers are summarized in Table I. The inherent viscosity of the PEO-*r*-PPO_{2500}-T6T6T copolymer was 1.03 dL/g, which indicated the successful formation of a high-molecular weight material.

Differential scanning calorimetry

The melting behavior of the copolymers was investigated with DSC and the data obtained from the second heating scan was used in order for the thermal history of the polymer not to have an influence (Table I). The SS melting temperature with PEO_{2000} segments was 21°C and that of the polymers with PEO-*r*-PPO segments was −13°C. The copolymers with PPO did not display a polyether melting transition. The heat of fusion per weight of PEO was high for PEO_{2000} and much lower for PEO-*r*-PPO_{2500}. Copolymerization of PEO with PPO units decreased the PEO melting temperature and crystallinity; however, the PEO-*r*-PPO_{2500} segments were not fully amorphous. Nevertheless, the values of the PEO melting temperature and the heat of fusion of the copolymers with PEO-*r*-PPO were much lower than the corresponding values of a PEO/PPO mixture with 81 wt % PEO.[18]

The T6T6T melting temperature in the copolymers were all high and the highest value was found for PPO_{2300}-T6T6T. The T6T6T melting temperature in the copolymer is dependant on the solvent effect of the polyether segments,[5] which suggests that the PEO segments presented a stronger interaction with T6T6T as opposed to their PPO counterparts. The heat of fusion values of T6T6T segments were all moderately high.

Fourier transform infrared spectroscopy

A specific method for studying the crystallinity of amide segments in copolymers is FTIR spectroscopy.[5,29,30] The wave number of the amide carbonyl absorbance band is sensitive to the H-bonding strength, and for T6T6T, in the crystalline state, this occurred at 1627 cm^{-1}, whereas the corresponding wavelength in the amorphous state is $\sim$ 1665 cm^{-1}. The wave number of the ester carbonyl band was 1720 cm^{-1}, and this ester band was found not to be

TABLE I
Selected Properties of Block Copolymers with T6T6T and PEO2000, PEO-*r*-PPO2500, and PPO2300 Segments

			PEO		DSC				DMA			FTIR	Water absorption
					PEO		T6T6T						
Polymer	SS Mol wt (g/mol)	HS (wt %)	Copol (wt %)	SS[a] (mol %)	η_{inh} (dl/g)	T_g (°C)	T_m (°C)	ΔH_m, (J/g·PEO)	T_m (°C)	ΔH_m (J/g·T6T6T)	T_g (°C)	T_{flex} (°C)	$T_{m,T6T6}$ (°C)	$G'_{25°C}$ (MPa)	$X_{C,T6T6T}$ (%)	WA (wt %)
PEO[5]	2000	23.8	76.2	100	2.10	nm	21	53	176	73	−48	20	174	38	85	91
EO-PPO-EO[3]	2300	21.3	16	20	1.03	nm	am	am	190	45	−61	−50	194	28	75	nm
PEO-*r*-PPO	2500	20.0	60	75	0.92	−60	−13	16	163	57	−63	−15	170	24	80	85

nm: not measured; am: amorphous.

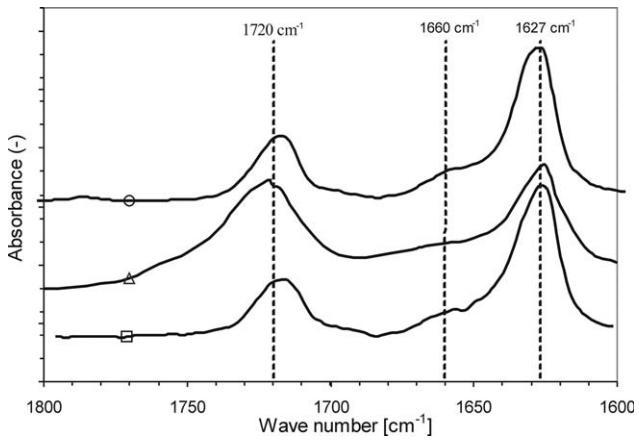

Figure 2 FTIR spectra of polyether-T6T6T in the 1800–1600 cm^{-1} range: ○, PEO; △, PPO; □, PEO-*r*-PPO.

sensitive to the packing of the chains.[5,29,30] The FTIR spectra of the copolymers are given in Figure 2.

The T6T6T copolymers all presented a very strong crystalline carbonyl band at 1627 cm^{-1} and only a very small amorphous carbonyl band at 1660 cm^{-1}. The amide carbonyl bands indicated that almost all the T6T6T was in the crystalline state. From the intensities of the crystalline and the amorphous amide peaks, the T6T6T crystallinity in the copolymers could be calculated according to eq (1) (Table I). The T6T6T crystallinities for the copolymers were all high and little dependent on the type of the polyether.

Dynamic mechanical thermal analysis

The thermal mechanical properties were analyzed by dynamic mechanical thermal analysis (DMTA), and Figure 3 displays the storage modulus (G') as a function of temperature. The corresponding data are summarized in Table I.

As can be observed in the DMTA graphs, three transitions were present: a glass transition of the

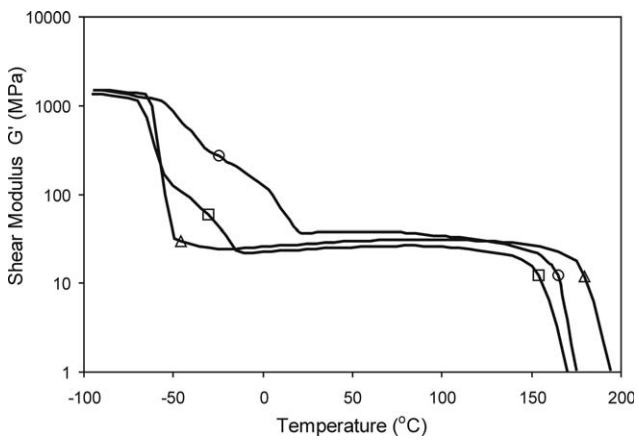

Figure 3 The shear modulus of polyether-T6T6T as a function of temperature for: ○, PEO_{2000}; △, PPO_{2300}; □, PEO-*r*-PPO_{2500}.

polyether phase, a melting transition of the PEO crystallites, and a melting transition of the T6T6T crystallites. The PEO_{2000}-T6T6T copolymer displayed a T_g of $\sim -48°C$ and a shoulder before the start of the rubbery plateau. This shoulder was due to the melting of the PEO crystallites, and its height was related to the PEO crystallinity.[18] The start of the rubbery plateau (T_{flex}) (20°C) corresponded to the PEO melting temperature (21°C) as measured by DSC (Table I). This PEO melting temperature was relatively high and hampered the low-temperature elastic behavior. The shear modulus at the rubbery plateau was nearly constant with temperature—a behavior that is typical for copolymers with monodisperse HS—and was due to the fact that all the T6T6T segments melted at a single temperature.[3,5,29]

Poly(propylene oxide) segments are known not to crystallize and this was also the case for the EO-PPO-EO segments.[3,18] The PPO_{2300}-T6T6T copolymers displayed two transitions: a T_g for the PPO phase and a T_m for the T6T6T crystallites (Fig. 3).

The T_g for the PPO phase was low (−61°C) and the transitions sharp. As there was no crystalline polyether phase present, the start of the rubbery plateau (T_{flex}) occurred at a very low temperature (−50°C), and this low value of T_{flex}, indicates an excellent low temperature flexibility of the PPO_{2300}-T6T6T copolymers.[3] The modulus of this copolymer in the rubber region was slightly lower that that for PEO, which was explained by the slightly lower T6T6T concentration. The flow transition corresponded to the melting temperature of the T6T6T segments as measured by DSC and was for PPO_{2300}-T6T6T found to be 20°C higher than for PEO_{2000}-T6T6T. The higher T_m with PPO as compared to PEO was due to the lower interaction of the PPO with amide segments.[18]

The PEO-*r*-PPO_{2500}-T6T6T copolymer had a T_g of −63°C that was slightly lower than for the copolymer with PPO segments. The presence of merely 25 wt % of PPO in PEO-*r*-PPO had a strong effect on the T_g. The copolymer with PEO-*r*-PPO_{2500} segments displayed a small shoulder of the PEO crystalline phase at temperatures above their T_g. This shoulder was smaller than for the copolymer with PEO_{2000}, and the value of T_{flex} (PEO melting temperature) was also lower. The crystalline order of the PEO in PEO-*r*-PPO was reduced due to the presence of the PPO units, but the segments were not fully amorphous. The PEO-*r*-PPO_{2500} copolymer had clearly improved low temperature properties as compared to PEO_{2000}, and in comparison to the copolymer with a PEO/PPO mixtures and 81 wt % PEO,[18] the values of PEO T_g and T_{flex} were much lower.

The shear modulus at room temperature is known to be highly dependant on the HS concentration.[29,30] The modulus of the polyether-T6T6T copolymers decreased when going from PEO to PPO to PEO-*r*-PPO. This was probably due to the lowering of the T6T6T concentration (Table I).

The modulus in the rubber plateau increased somewhat with increasing temperatures; a behavior typical of ideal elastomers that has been observed earlier for segmented copolymers with monodisperse HS.[3,5,29,31] The flow temperatures corresponded to the melting temperature of the T6T6T segments

Water absorption

The WA values for the copolymers with PEO and PEO-*r*-PPO segments were high (Table I). The WA of PPO_{2200}-T6T6T could not be measured as no sample was left; however for the similar PPO-diaramide, the WA was found to be 14%.[5] It was thus believed that the corresponding value for PPO_{2300}-T6T6T should be similar or even lower. The PPO segments (with 20 wt % EO end units) were much less hydrophilic than the PEO-*r*-PPO material with 25 wt % PPO units. The PPO groups in PEO-*r*-PPO thus seemed to have a small effect on the WA. The WA values were similar to those of the copolymer with a mixture of PEO/PPO and 81 wt % PEO.[5]

Influence PEO-*r*-PPO segment length

Generally, segmented copolymers with low concentrations of HSs demonstrate extremely low moduli, decent low-temperature properties, and excellent elastic behaviors. A low HS concentration can be obtained by using short HSs and/or long SSs. However, segmented block copolymers with long SSs (>3000 g/mol) often experience the problem of liquid–liquid demixing —a morphology that is most often unwanted. Liquid–liquid demixing is particularly strong for polyurethanes and poly(ether-amide) segmented block copolymers,[32] Nevertheless, it is possible to avoid it in the latter by using short monodisperse polyamide segments.[3,5,17,18,31]

Studies were performed on the synthesis of the PEO-*r*-PPO_{12000}-T6T6T copolymer. By using very long PEO-*r*-PPO_{12000} segments, the melt was opaque during the synthesis and the copolymer had a low molecular weight. However, if PEO-*r*-PPO_{2500} was extended with terephthalate groups, even to a segment length of 10,000 g/mol, the melts stayed transparent and copolymers with elevated molecular weight were obtained (Table II). A similar behavior has been observed previously.[26–29] Moreover, the effect of the PEO-*r*-PPO segment length on the properties of the PEO-*r*-PPO-T6T6T copolymers was explored. All the studied copolymers were transparent in the melt and in the solid state. The

TABLE II
Selected Properties of (PEO-*r*-PPO$_{2500}$)$_y$-T6T6T Segmented Block Copolymers

Polymer	SS Mol wt (g/mol)	HS (wt %)	PEO Copol (wt %)	PEO SS[a] (mol %)	η_{inh} (dl/g)	DSC PEO T_g (°C)	DSC PEO T_m (°C)	DSC PEO ΔH_m, (J/g$_{\cdot PEO}$)	DSC T6T6T T_m (°C)	DSC T6T6T ΔH_m (J/g$_{\cdot T6T6T}$)	DMA T_g (°C)	DMA T_{flex} (°C)	DMA $T_{m_{T6T6T}}$ (°C)	DMA $G'_{25°C}$ (MPa)	FTIR $X_{C_{T6T6T}}$ (%)	Water absorption WA (wt %)	Water absorption ϕ (–)	Water absorption CA (°)
PEO-*r*-PPO	1000	38.4	46.2	75	0.85	–52	am	am	183	49	–53	–35	212	77	81	30	0.23	39
(PEO-*r*-PPO-T)	2500	20.0	60	75	0.92	–60	–13	16	163	57	–63	–15	170	24.2	80	85	0.46	25
	3750	14.2	64	74	0.77	–59	–5	30	151	63	–59	–10	151	13.9	85	89	0.47	22
	5000	11.0	64	72	1.09	–60	–6	29	147	46	–60	–10	147	8.5	81	113	0.53	22
	7500	7.3	66	71	1.22	–60	–5	33	149	35	–60	–5	144	4.9	76	123	0.55	21
	10000	5.6	67	71	1.56	–60	–6	33	144	32	–60	–5	143	3.9	65	128	0.56	nm

nm: not measured; am: amorphous.

copolymers displayed high values of inherent viscosity suggesting high molecular weights.

Differential scanning calorimetry

DSC analyses of the PEO-*r*-PPO-T6T6T copolymers revealed three transitions: a T_g of the polyether phase, a T_m of the PEO units, and a T_m of the T6T6T segments (Fig. 4).

The T_g of the copolymers did not change when the SS length was increased from 2500 to 10,000 g/mol (Table II). In fact, two effects could be observed for this series: a reduced crosslink density and an increased terephthalate concentration, and these two opposing effects seemed to cancel each other out. The PEO-*r*-PPO$_{1000}$ material had a T_g that was 10°C higher than the PEO-*r*-PPO$_{2500}$ because of the shorter ether segment length.[5]

The PEO-*r*-PPO$_{1000}$ had no PEO melting temperature, and the copolymers with 2500–10,000 g/mol SS presented a PEO crystallization peak followed by a melting peak upon heating. The PEO melting temperature of copolymers was found to increase slightly with the SS length. The heat of fusion values also increased with the SS length, suggesting that the PEO in the terephthalate-extended segments possessed a higher crystallinity as well as a crystalline phase that melted at a slightly higher temperature. However, for pure PEO segments with a high molecular weight, the crystallinity and melting temperature were much higher.[5]

The T6T6T melting temperatures in these copolymers decreased with an increasing SS length (Table II). The T_m of the HS is known to become reduced with an increasing polyether concentration, and this was explained by a solvent effect of the polyether segments.[31] At very low T6T6T concentrations, the heat of fusion of these segments was difficult to determine, but the obtained results suggested a

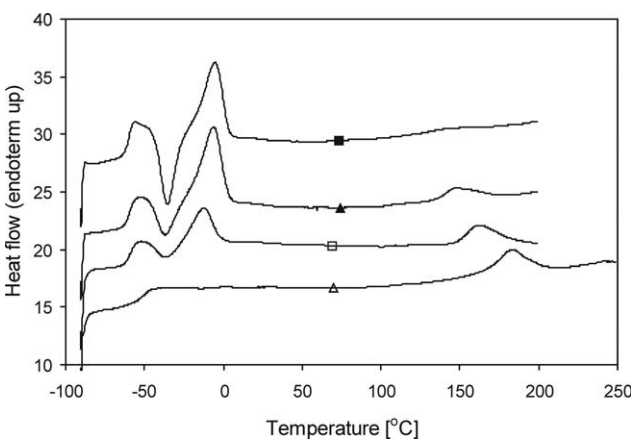

Figure 4 DSC results of the PEO-*r*-PPO-T6T6T copolymers: △, 1000; □, 2500; ◆, 5000; ■, 10,000.

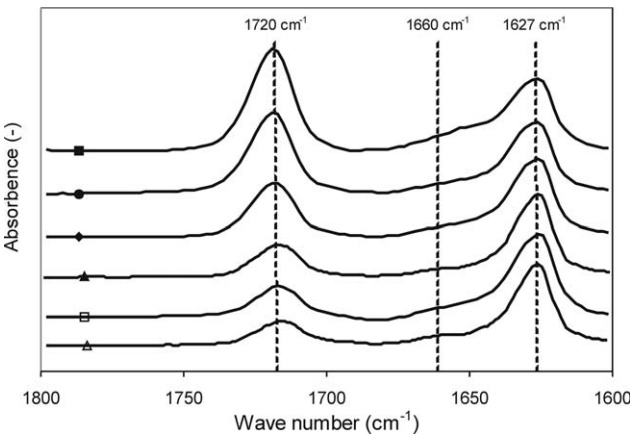

Figure 5 FTIR spectra of the PEO-*r*-PPO-T6T6T copolymers: △, 1000; □, 2500; ▲, 3750; ◆, 5000; ●,7500; ■, 10,000.

lower T6T6T crystallinity at low T6T6T concentrations.

Fourier transform infrared spectroscopy

The crystallinity of the T6T6T segments was studied with FTIR, and the crystalline amide peaks (1627 cm^{-1}) were visible even at very low amide concentrations (Fig. 5).

By extending the PEO-*r*-PPO with terephthalate groups, the intensity of the ester carbonyl peaks increased as compared to the amide peaks. The position of the crystalline amide band at 1627 cm^{-1} and the amorphous amide band at 1665 cm^{-1} did not shift upon altering the composition. The T6T6T crystallinities were determined based on the peak intensities of the crystalline and amorphous amide bands in combination with eq (1), and the results are presented in Table II. The crystallinity of the T6T6T segments was found to be remarkably high in all samples (65-80%), and for the copolymers with very low T6T6T concentrations, the crystallinities determined by this method were more reliable than those obtained with DSC.

Atomic force microscopy analysis

T6T6T crystallites are know to present a nano-ribbon morphology,[26,33] and this morphology can be visualized best at very low concentrations of mono disperse segments.[29,34] The morphology of (PEO-*r*-PPO_{2500}-T)$_{10000}$-T6T6T was studied by AFM on solvent cast films with thicknesses of either 20 μm or 100 μm. Films with 20-μm thicknesses are normally used for AFM analysis, and the surface structure in the 20-μm film was found to correspond to that of an amorphous matrix in which were dispersed nano-ribbon crystallites [Fig. 6(A)].

The ribbons have three dimensions a thickness, a width, and a length. These ribbons all appeared to have similar widths (thicknesses) suggesting that their widths and thicknesses were approximately the same. The ribbons were long (more than 500 nm), presented a high aspect ratio, and were dispersed like spaghetti in a dish. However, they were not ordered into spherulites.

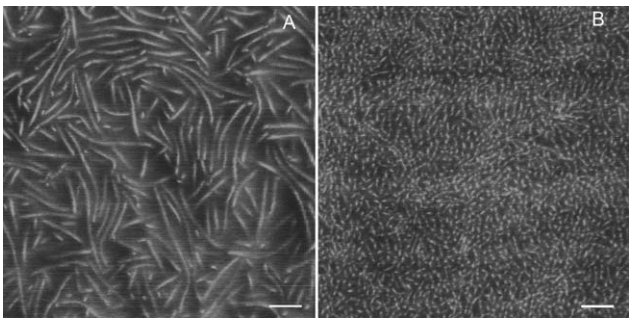

Figure 6 AFM micrographs of (A) a thin (20 μm) and (B) a thick (100 μm) (PEO-*r*-PPO_{2500}-T)$_{10,000}$-T6T6T sample.

The AFM micrograph of a 100-μm-thick sample of the same material had a completely different appearance [Fig. 6(B)]. In this thick sample, numerous dots that seemed to be rectangular were seen instead of ribbons. It was illogical to think that the T6T6T had not crystallized into ribbons, and thus the observed dots were believed to be ribbons oriented perpendicular to the surface. Figure 6B thus displays the cross section of the ribbons. Although the amide concentration was only 5.6 wt %, crystalline ribbons were clearly present. However, why the ribbons in the thicker sample were oriented differently as opposed to in their thinner counterpart remains unknown.

Dynamic mechanical thermal analysis

The thermal mechanical properties of the materials were analyzed by DMTA, and Figure 7 displays the shear storage modulus (G') as a function of the

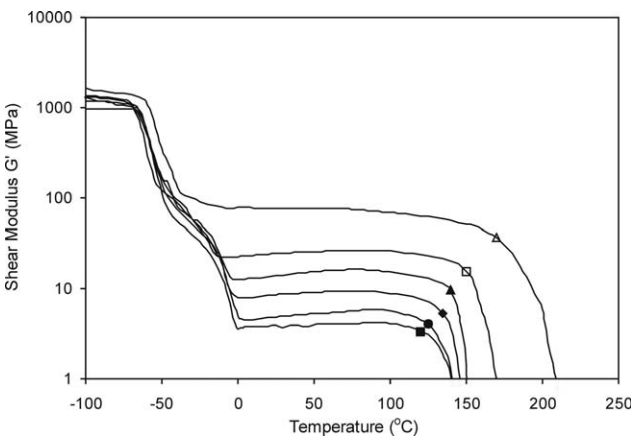

Figure 7 The shear storage modulus G' as a function of the temperature for PEO-*r*-PPO-T6T6T copolymers: △, 1000; □, 2500; ▲, 3750; ◆, 5000; ●,7500; ■, 10,000.

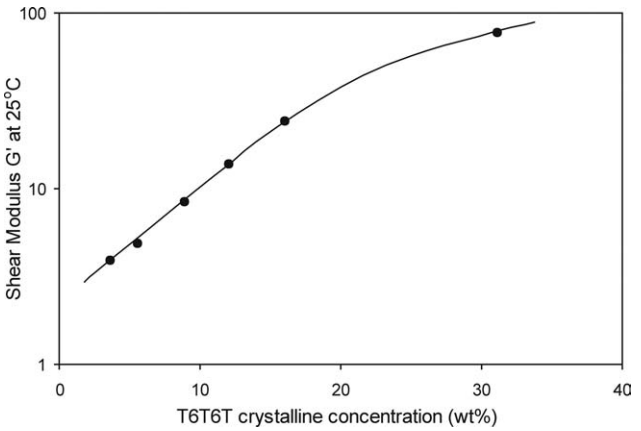

Figure 8 The shear modulus for the (PEO-*r*-PPO_{2500}-T)$_y$ copolymers as a function of the crystalline T6T6T concentration.

temperature. The corresponding data are summarized in Table II.

As can be observed in the DMTA graphs, three transitions were present: a glass transition of the polyether phase, a melting transition of the PEO crystallites, and a melting transition of the T6T6Tsegments. The glass transition occurred at a low temperature (−60°C) and remained unchanged as the segment length was increased from 2500 to 10,000 g/mol.

In the slope of the T_g, a shoulder that was due to the PEO melting can be seen. This shoulder was, however, absent for the PEO-*r*-PPO_{1000} copolymer, as a result of this short ether segment being amorphous, as demonstrated by the DSC results. Because of the absence of a crystalline ether phase, the rubber plateau for this copolymers started at a low temperature (−35°C). For the other copolymers, the rubber plateau started in the range of −15°C to −5°C (T_{flex}). The T_{flex} shifted to slightly higher temperatures with an increasing (PEO-*r*-PPO_{2500}-T)$_y$ length in a similar way to the change in PEO melting temperature as observed by DSC (Table II). Up to a temperature of −20°C in the DMTA graph, the moduli of the copolymers seemed to present identical values despite the decreasing modulus at room temperature. The low temperature properties of the (PEO-*r*-PPO_{2500}-T)$_y$-T6T6T copolymers did not improve with increasing the (PEO-*r*-PPO_{2500}-T)$_y$ segment length. Rather, the PEO T_m was found to be somewhat higher.

At room temperature, which is above the PEO melting temperature, the modulus decreased strongly with an increasing SS length (decreasing T6T6T concentration) (Table II).[5] Because of the modulus of the rubber plateau being a function of the reinforcing effect of the T6T6T crystallites, the modulus was plotted as a function of the T6T6T crystalline concentration (T6T6T concentration × T6T6T crystallinity as measured by FTIR) (Fig. 8).

There was a significant increase in the log modulus with the T6T6T crystalline concentration, and this behavior was similar to that of other segmented block copolymers with T6T6T segments.[5,29] All these copolymers had nano-ribbon crystallite structures of the T6T6T segments, which acted as physical crosslinks as well as reinforcing fillers in the materials. The observed increase in modulus in the segmented block copolymers could thus be described by a fiber-reinforced composite model.[3,29]

The shear modulus in the temperature range from room temperature to near the melting temperature was nearly constant and the modulus even seemed to increase slightly. This ideal rubber behavior is typical for copolymers with monodisperse HS.[3,5,18,29] Upon melting of the T6T6T crystallites, the polymer started to flow and the flow transition temperatures (T_{flow}) decreased with an increasing SS segment length, similarly to the T_m as measured by DSC (Table II). The decrease in T6T6T melting temperature with the SS concentration for the PEO-*r*-PPO resembled that of the PEO_x copolymers (Fig. 9).

The HS melting temperature is known to decrease with increasing polyether concentration as well as with an increasing polyether-polyamide interaction, and this decrease has been explained as the result of a solvent effect of the polyether segments.[3,5,18,29,31]

Water absorption

The T6T6T segments in the polyether-T6T6T copolymers are the physical crosslink points and the polyether segment length the length between crosslink points, which is inversely related to the crosslink density. By increasing the molecular weight of the SS segments, the T6T6T concentration, and consequently also the crosslink density, was lowered. A lower crosslink density allows more swelling and thus an increased WA.[35] Another expected effect

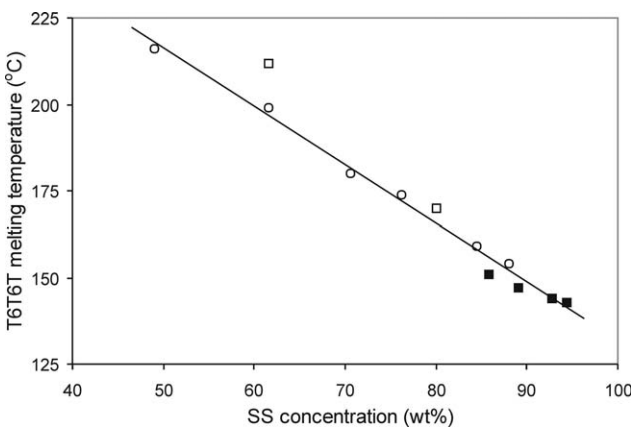

Figure 9 The T6T6T melting temperature as a function of the SS concentration: ○, PEO_x[5]; □, PEO-*r*-PPO_x; ■, (PEO-*r*-PPO_{2500}-T)$_y$.

was that the hydrophobic terephthalate groups in the polyether should slightly reduce the WA of the copolymers.[36] The WA values were high and increased with the (PEO-*r*-PPO_{2500}-T)$_y$ segment length (Table II). Because the water concentration in the swollen copolymer was expected to be a function of the crosslink density, the values were plotted as functions of the reciprocal molecular weight of the segments (Fig. 10).[35]

The water concentration in the swollen copolymers increased linearly with a decreasing crosslink density, and the values for the (PEO-*r*-PPO_{2500}-T)$_y$-T6T6T were lower than for PEO_x-T6T6T. This was mainly due to the presence of the PPO groups, whereas the terephthalic groups in (PEO-*r*-PPO_{2500}-T)$_y$ seemed to have very little effect.

Contact angles

Copolymers containing PEO segments often have low CAs, and their values generally decrease with an increasing PEO segment length.[19] The CAs were measured on wetted melt-pressed films using the static CB method, and the angles were determined by manual evaluation mode. For these hydrophilic copolymers, the CB method provided reproducible results. As the SS flexibility depended on the crosslink density, the CAs of the PEO-*r*-PPO-T6T6T copolymers are given in Figure 11 as functions of the reciprocal SS molecular weight.

The CAs of PEO-*r*-PPO-T6T6T were very low and, as can be seen, they decreased with a decreasing reciprocal SS molecular weight (crosslink density). This decrease was linear and both the PEO-*r*-PPO-T6T6T and (PEO-*r*-PPO-T)$_y$-T6T6T materials followed this trend. The terephthalic groups did not display any specific effect. Extrapolation of the CA values to very long SS led to a value of $\sim 20^\circ$.

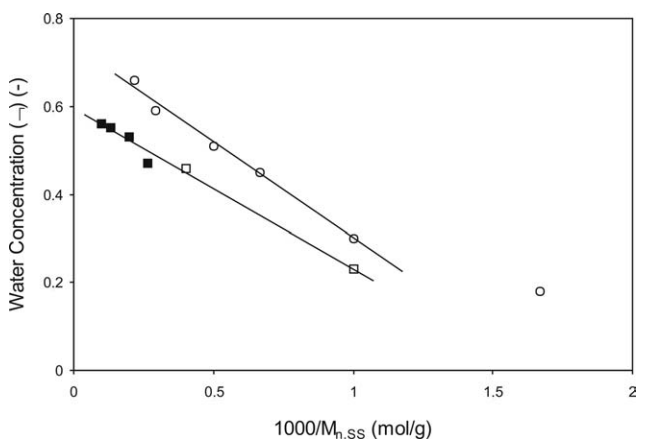

Figure 10 The water concentration in the polyether-T6T6T copolymers as a function of the reciprocal polyether segment length (crosslink density): ○, PEO_x [36]; □, PEO-*r*-PPO_x; ■, (PEO-*r*-PPO_{2500}-T)$_y$.

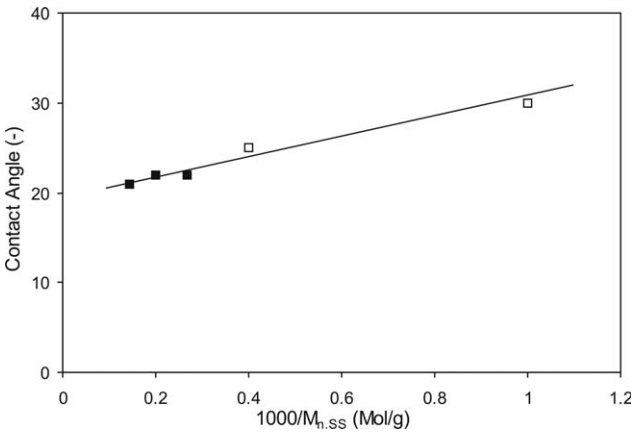

Figure 11 Contact angles as functions of the reciprocal polyether molecular weight (crosslink density): ○, PEO_x[19]; □, PEO-*r*-PPO_x; ■, (PEO-*r*-PPO_{2500}-T)$_y$.

CONCLUSIONS

Segmented block copolymers with PEO-*r*-PPO_{2500} segment were prepared and short monodisperse T6T6T with a high crystallinity were chosen as the HS. As compared to the PEO segments, the PEO-*r*-PPO_{2500} displayed both a lower crystallinity and a lower melting temperature. The presence of 25% PPO in these segments slightly decreased the WA values, and also the glass transition temperature was reduced. The highly crystalline T6T6T segments presented a morphology consisting of nano-ribbons with high aspect ratios. These ribbons reinforced the polyether soft phase in a significant manner.

Extending the PEO-*r*-PPO_{2500} segments with terephthalic groups increased the PEO crystallinity and melting temperature and modified the low-temperature properties of the copolymer somewhat. However, the room-temperature modulus could be lowered while simultaneously increasing the hydrophilicity and decreasing the contact angle to very low values.

Ultimately, as compared to mixtures of PEO/PPO, a random dispersion of PPO units in the PEO segments (i.e., PEO-*r*-PPO) was more effective in reducing the PEO crystallinity and melting temperature, without affecting the hydrophilicity.

The authors wish to express their gratitude to Mrs. H. ten Hoopen for performing the AFM analysis.

References

1. Holden, G.; Legge, N. R.; Quirk, R.; Schroeder, H. E. Thermoplastic Elastomers; Hanser: Munich, 1996.
2. Fakirov, S. Handbook of Condensation Thermoplastic Elastomers; Wiley: New York, 2005.
3. Van der Schuur, J. M.; Gaymans, R. J. J Polym Sci Part A: Polym Chem Ed 2006, 44, 4769.
4. Niesten, M. C. E. J.; Gaymans, R. J. Polymer 2001, 42, 6199.

5. Husken, D.; Feijen, J.; Gaymans R. J. J Polym Sci Part A: Polym Chem Ed 2007, 45, 4522.
6. Schneider, N. S.; Langlois, D. A.; Byrne, C. A. Polym Mater Sci Eng 1993, 69, 249.
7. Schneider, N. S.; Illinger, J. L.; Karasz, F. E. Polymers of Biological and Biomedical Significance; American Chemical Society: Washington D.C., 1994.
8. Lee, D.; Lee, S.; Kim, S.; Char, K.; Park, J. H.; Bae, Y. B. J Polym Sci Part B: Polym Phys 2003, 41, 2365.
9. Chen, C. T.; Eaton, R. F.; Chang, Y. J.; Tobolsky, A. V. J Appl Polym Sci 1972, 16, 2105.
10. Schneider, N. S.; Illinger, J. L.; Karasz, F. E. J Appl Polym Sci 1993, 47, 1419.
11. Yilgör, J.; Yilgör, E. Polymer 1999, 40, 5575.
12. Gebben, B. J Membr Sci 1996, 113, 323.
13. Stroeks, A.; Dijkstra, K. Polymer 2001, 42, 117.
14. Metz, S. J.; Mulder, M. H. V.; Wessling, M. Macromolecules 2004, 37, 4590.
15. Deschamps, A. A.; Grijpma, D. W.; Feijen, J. Polymer 2001, 42, 9335.
16. Bondar, V. I.; Freeman, B. D.; Pinnau, I. J Polym Sci Part B: Polym Phys 1999, 37, 2463.
17. Bondar, V. I.Freeman, B. D.; Pinnau, I. J Polym Sci Part B: Polym Phys 2000, 38, 2051.
18. Arun, A.; Gaymans, R. J. Eur Polym 2009, 45, 2858.
19. Husken, D.; Feijen, J.; Gaymans, R. J. J Appl Polym Sci 2009, 114, 1264.
20. Husken, D.; Gaymans, R. J. J Appl Polym Sci 2009, 112, 2143.
21. Husken, D.; Visser, T.; Wessling, M.; Gaymans, R. J. J Memb Sci 2010, 346, 194.
22. Park, J. H.; Bae, Y. H. J Appl Polym Sci 2003, 89, 1505.
23. Park, J. H.; Cho, Y. W.; Kwon, I. C.; Jeong, S. Y.; Bae, Y. H. Biomaterials 2002, 23, 3991.
24. Shibaya, M.; Suzuki, Y.; Doro, M.; Ishihara, H.; Yoshihara, N.; Enomoto, M. J Polym Sci Part B: Polym Phys 2006, 44, 573.
25. Husken, D.; Feijen, J.; Gaymans, R. J. Eur Polym J 2008, 44, 130.
26. Niesten, M. C. E. J.; ten Brinke, J. W.; Gaymans, R. J. Polymer 2001, 42, 1461.
27. Krijgsman, J.; Husken, D.; Gaymans, R. J. Polymer 2003, 44, 7573.
28. Husken, D.; Feijen, J.; Gaymans, R. J. Macromol Chem Phys 2008, 209, 525.
29. Arun, A.; Dullaert, K.; Gaymans, R. J. Macromol Chem Phys 2009, 210, 48.
30. Biemond, G. J. E.; Feijen, J.; Gaymans, R. J. J Appl Polym Sci 2007, 105, 951.
31. Arun, A.; Gaymans, R. J. Macromol Chem Phys 2008, 209, 854.
32. Niesten, M. C. E. J.; Feijen, J.; Gaymans, R. J. Polymer 2000, 41, 8487.
33. Van Der Schuur, M. J.; van der Heide, E.; Feijen, J.; Gaymans, R. J. Polymer 2005, 46, 3616.
34. Biemond, G. J. E.; Feijen, J.; Gaymans, R. J. Macromol Mater Eng 2009, 294, 492.
35. Sauer, B. B.; McLean, R. S.; Gaymans, R. J.; Niesten, M. C. E. J. J Polym Sci Part B Polym Phys 2004, 42, 1783.
36. Flory, J. P.; Rehner, J. J Chem Phys 1943, 11, 521.
37. Husken, D.; Gaymans, R. J. Macromol Chem Phys 2008, 209, 967.